The Variation of Flow Stress with Substructure in Tantalum

Walter S. Owen
Department of Metallurgy
University of Liverpool.

1. General Features

On annealing cold worked (90 percent reduction at 20°C) tantalum (less than 160 ppm total interstitial impurity) at successively higher temperatures four effects were observed[1]. In order of increasing annealing temperature:

1. The dislocation density of the cold-worked foils was very high (greater than 3×10^{11} cm^{-2}). It was difficult to resolve the individual dislocations and no clear cell structure was observed. On annealing for 30 minutes at 900°C there was some rearrangement and annihilation of dislocations but no formation of sub-boundaries. The density decreased to about 9×10^{10} cm^{-2}.

2. Annealing at temperatures between 950° and 1200°C produced sub-boundary networks which were very regular at the higher temperatures in the range (Figure 1). More than 60 percent of the networks were of the ⟨111⟩/⟨100⟩ type.

3. At higher annealing temperatures coarser networks were produced, corresponding to a decrease on the angular misorientation across the boundary. There was a small decrease on the average dislocation density.

4. No networks were found in specimens annealed at still higher temperatures (up to 1700°C) and there was a very marked decrease in the average dislocation density.

The processes overlap somewhat and the annealing temperature at which each effect was observed varied appreciably with the purity of the tantalum. In the most impure material (147 ppm oxygen, 160 ppm total impurity) effects 2 and 4 occurred at the lowest temperatures and the average dislocation density decreased most rapidly with increasing annealing temperature.

2. The Change of Substructure on Deforming Annealed Foils in Tension

The sequence of changes in the substructure on deforming annealed foils in tension at constant temperature is similar to those observed in iron[2,3,4], but there are differences in detail.

After 1.6 percent strain at 293°K many straight dislocations were observed and the start of network disintegration was detected in relatively pure tantalum (Ta-E1 containing less than 35 ppm total interstitial impurity) with a high initial dislocation density (5×10^{10} cm^{-2}). In the annealed specimen most of the dislocations were in well developed networks although there were an appreciable number of random dislocations. Very few regular networks remained after 2.0 percent strain and a number of tangles of dislocations had formed. There was some indication of cell formation although it was not possible to estimate the cell size. After 4.6 percent strain the cell structure was better defined, the cell diameter being about 0.3μ, and there were extensive dislocation tangles. The cells were clearly defined after 7.3 percent strain and the diameter was about 0.2μ(Figure 2). However, unlike iron deformed at the same temperature, after further strain the cells started to break-up. Although some evidence of cells remained after 10.6 percent strain the dislocation distribution was much more uniform than after 9.2 percent. After 12.2 percent strain the cell structure had disappeared and the dislocation density was uniform throughout the specimen (Figure 3).

The strain at which tangles and cells form is greatly influenced by the initial substructure. A dilute tantalum-oxygen alloy (Ta-E4 containing 147 ppm oxygen) annealed to give a low dislocation density (1×10^{9} cm^{-2}) arranged randomly showed only slight evidence of cell formation after 10.0 percent strain at 293°K although there was a marked increase in the dislocation entanglement (Figure 4). This contrasts with the same alloy annealed to a high dislocation density, with all the dislocations in well-formed networks, which proved remarkably resistant to disintegration on straining. Even after 11.0 percent strain some of the original networks could still be observed. In Figure 5 a network surviving after 6.7 percent strain is shown. Although the network is still intact the surrounding areas show obvious signs of deformation. Thus, it seems that, in general, high dislocation density specimens form tangles and subsequently cells more readily than those with low initial density, but annealed-in networks vary significantly in their ability to withstand disintegration. Comparing the general deformation structures in tantalum with those described for iron[2-4] it seems that tantalum deformed at 293°K corresponds to iron deformed at a temperature 100°K or more higher. Since the melting point of tantalum is appreciably higher than that of iron this difference is not surprising.

Several sources of dislocation multiplication have been identified. Profuse generation of dislocations has been observed in the vicinity of the

intersection of a slip band with a dislocation network (Figure 6). It seems that when a network is broken up by a slip band cutting through it many new dislocations are produced. In addition, it was observed in all the specimens that as the deformation was increased the grain boundaries became thicker and more fuzzy due to the accumulation of dislocations along the boundary (Figure 7). It is not clear where these dislocations originate but it seems unlikely that they are formed by the blocking of a slip band because when this occurs the new dislocations can be clearly seen and they are more widely dispersed (Figure 8).

3. The Variation of Flow Stress with Dislocation Density

The average dislocation density was measured, by the method described by Keh and Weissman[4], as a function of flow stress for two specimens of Ta-E4 with the same grain size, one (Ta-E4 LD) with a low (1×10^{9} cm^{-2}) and the other (Ta-E4 HD) with a high density of dislocations (1.6×10^{10} cm^{-2}). In the low density material the dislocations were random and in that with a high dislocation density almost all of the dislocations were in well-developed networks. The mechanical and thermal treatments are given in Table 1. Ta-E4 LD was tested at 293°K, and 240°K and the other specimens at 293°K only.

The stress-strain curves are shown in Figure 9. As with all polycrystalline dilute tantalum alloys tested in this and other investigations the logarithm of the true stress σ varied linearly with the logarithm of the true strain ε when the strain was greater than the Luders strain. Thus, the strain-hardening curve could be accurately represented by:-

$$\sigma_f = K \varepsilon^n \qquad (1)$$

where K is the strength constant and n the strain-hardening index. Values of the flow stress at zero plastic strain σ_{fo} were obtained by logarithmic extrapolation of the strain hardening curve to the intersection with the elastic line[5,6]. Values of the lower yield stress σ_y, σ_{fo}, K and n are listed in Table 1. Changing the initial substructure (compare Ta-E4 LD and Ta-E4 HD) produces only a very small difference in the yield stress at 293°K but the difference in σ_{fo} is appreciable. Clearly, σ_{fo}, K and n are markedly affected by the initial substructure. Many determinations of σ_i, which is equivalent to σ_{fo}[6], have been made on other materials using the Petch extrapolation which depends on

$$\sigma_y = \sigma_i + k_y d^{-\frac{1}{2}} \qquad (2)$$

where 2d is the grain size and k_y a locking parameter. This method cannot be used to study the effect of substructure on the yield parameters because of the practical difficulty of maintaining a constant dislocation arrangement

and density in a series of specimens with an appreciable range of grain size. When the grain size range is established by annealing cold-worked tantalum at successively higher temperatures the Petch method measures some averaged value of σ_i which is higher than σ_{fo} measured by extrapolation of the strain hardening curve[5]. In iron specimens, which usually go through a phase change during the annealing to establish the grain size, the variation of substructure with annealing temperature is not marked and there is good agreement between σ_i by the Petch method and σ_{fo} by extrapolation of the strain-hardening curve[7].

Following Keh and Weissman[4] the flow stress for Ta-E4 LD and Ta-E4 HD was plotted as a function of $\sqrt{N}$, where N is the average dislocation density, and all the tantalum specimens were found to approximate to the empirical relationship

$$\sigma_f = \sigma_o + \alpha G b \sqrt{N} \qquad (3)$$

where σ_o and α are constants, G is the shear modulus and b the Burgers vector (Figure 10). A relationship of this form is predicted by several different strain hardening theories but the models on which the theories are based relate to the second stage of linear hardening of a single crystal and the extension of these ideas to the non-linear hardening of polycrystals is of doubtful significance. Further, to interpret equation 3 in these terms an assumption is necessary about the fraction of dislocations which are mobile or the ratio between the dislocation density of the tangled regions and the average density. In polycrystalline tantalum specimens the dislocation geometry changes markedly with the preliminary mechanical and thermal treatment and with strain during testing and thus a simple assumption of this type does not appear to be justified. The problem has been discussed in detail by Keh and Weissman[4]. However, equation 3 is a useful empirical representation of the results and it enables the flow stress at zero strain σ_{fo} to be obtained by a third method. σ_{fo} is the stress corresponding to the initial dislocation density N_i. Values of σ_{fo} obtained in this way are given in Table 1. The values from equation 3 are a little greater than those from the stress-strain curve but the agreement is fair.

The variation of average dislocation density with strain could be represented by a simple power relationship (Figure 11)

$$N = C \varepsilon^a \qquad (4)$$

values of C and a are given in Table 1. A similar result has been found for iron and, by etch-pit counting, for mild steel[8]. Hahn replaces the total strain ε by the elastic strain ε_p, but as the elastic strain is small compared with ε over the range of the experimental measurements this substitution does not make a significant difference. Hahn[8] has advocated the use of

$$N - N_i = C' \varepsilon^{a'} \qquad (5)$$

The data for tantalum are plotted in this way in Figure 12. Each increment of strain is proportional to the number of moving dislocations N_m and the slip distance l, $\varepsilon = N_m b l$. At 293°K a or a' is nearly unity for both the high and low initial density specimens indicating that the product $N_m l/N$ is constant or, if the difference in the slip distance is assumed to be small, that the ratio of moving to static dislocations is independent of initial substructure. The fraction of dislocations moving can be assumed to be independent of the strain only if the slip distance is independent of the average dislocation density. At 240°K the situation is quite different, the strain varying approximately as the square root of the dislocation density. Thus, the product $N_m l/N$ varies with strain but without exact knowledge of the change in slip distance with strain and temperature no deduction about the effect of these variables on the fraction of dislocations moving can be made.

If equations 1 and 4 are judged to be a correct representation of the data then, eliminating ε,

$$\sigma_f = K C^{\frac{a-n}{n}} N^{\frac{n}{a}} \qquad (6)$$

Not surprisingly, since σ_f, N and ε are all taken from the same collection of interrelated data, the experimental results fit this relationship (Figure 13 and Table 1). Of course, equation 6 is not compatible with equation 3 since $\frac{n}{a} \neq 0.5$. The values of σ_{fo}, the stress corresponding to a dislocation density N_i, obtained from the data plotted in Figure 13 (equation 6) are given in Table 1. These are probably more reliable than those obtained from equation 3.

The Significance of σ_o

In the equation used by Keh and Weissman (equation 3) $\sigma_f = \sigma_o$ when $N = 0$ and σ_o might be considered to be the Peierls stress. However, σ_o defined in this way varies over a wide range when the initial substructure is changed (Figure 10 and Table 1). This, together with the objections to the application of this formula to polycrystalline material, suggests that no physical meaning can be given to this σ_o. Equation 6 is also unsatisfactory because neither of the equations from which it is derived (equations 1 and 4) take account of the Peierls stress. However, the fact that these equations appear to be a good representation of the experimental data indicates that the Peierls stress is small compared with σ_{fo}.

In the absence of a firmly-based equation relating the flow stress and the average dislocation density an attempt to assess the Peierls stress by a

more circuitous route appears justified. Previously, σ_{fo} has been defined as the point satisfying simultaneously equation 1 and the elastic equation

$$\sigma = E\varepsilon \tag{7}$$

where E is Young's modulus (Figure 14) and

$$\sigma_{fo} = K^{\frac{1}{1-n}} E^{\frac{n}{n-1}} \tag{8}$$

However, if it is assumed that σ_{fo} is the sum of two stresses, the Peierls stress σ_o and the stress σ_s required to move a dislocation through the annealed-in substructure, the relation between the elastic line and the strain-hardening curve may be as represented in Figure 15. σ_o is the strain introduced into the specimen by building up the dislocation density from zero to N_i. Hypothetically, if this is done without any dislocation interaction the stress required would be σ_o. Then, σ_{fo}, now defined as the stress at which the elastic line (equation 7) is tangential to the strain-hardening curve

$$\sigma_f - \sigma_o = K(\varepsilon - \varepsilon_o)^n \tag{9}$$

becomes

$$\sigma_{fo} = \sigma_o + K^{\frac{1}{1-n}} E^{\frac{n}{n-1}} n^{\frac{n}{1-n}} \tag{10}$$

Experimentally, the stresses σ_f and strains ε can be measured only at strains larger than the Luders strain. In these circumstances, if it is assumed that $\sigma_f \gg \sigma_o$ and $\varepsilon >> \varepsilon_o$ equation 9 reduces to equation 1 and n and K can be determined experimentally. Equation 1 fits the strain hardening curve very closely suggesting that at large strains this approximation is reasonable. The second term on the right-hand side of equation 10 differs from the right-hand side of equation 8 only by the factor $n^{\frac{n}{1-n}}$. For tantalum tested at 293°K n has values between 0.1 and 0.3 depending upon the initial substructure and $n^{\frac{n}{1-n}}$ varies between 0.77 and 0.60. Probably the least ambiguous method of determining σ_{fo} experimentally is from the data in Figure 13, taking σ_{fo} as the stress corresponding to N_i. Since the value from equation 8 (that is logarithmic extrapolation of the stress-strain curve) agrees fairly well with this value the decrease due to $n^{\frac{n}{1-n}}$ must be approximately compensated by the introduction of σ_o into equation 10. That is, between about 60 and 75 percent of σ_{fo} at 293°K is due to dislocation interaction.

Values of σ_o from the tantalum data obtained by taking σ_{fo} from the plots of ln σ_f versus ln N, and n and K from the application of equation 1 at large values of ε are given in Table 1. The values of σ_o for the high and low density specimens tested at the same temperature agree within the experimental error and it appears that further exploration of these ideas is justified.

The experimental results quoted in this paper are taken from work by Dr. D. Hull and Mr. I. McIvor which is still in progress. The work is supported by the United States Air Force under contract AF33(616) - 6838 Materials Laboratory, W.A.D.C., Wright-Patterson Air Force Base, Ohio; Manlabs Inc., Subcontract No. 105.

References

1. D. Hull, I. McIvor and W.S. Owen, J. Less Common Metals, 1962 (to be published).

2. W. Carrington, K.F. Hale, and D. McLean, Proc. Roy. Soc. 1960, 259A, 203.

3. D.G. Brandon and J. Nutting, J. Iron Steel Inst., 1960, 196, 160.

4. A.S. Keh and S. Weissman, Conference on the Impact of Transmission Electron Microscopy, California 1961

5. A. Gilbert, D. Hull, W.S. Owen and C.N. Reid, J. Less Common Metals, in press.

6. A.R. Rosenfield, J. Inst. Met. in press.

7. I. Mogford and D. Hull, private communication.

8. G.T. Hahn, Acta Met., 1962, 10, 727.

Table 1

	Ta-E4 LD		Ta-E4 HD
Treatment	Cold-worked 90 percent. Annealed 1750°C for 6 min.		Cold-worked 90 percent. Annealed 1750°C, 6 min. Cold worked 2 percent Annealed 1000°C, 1 hour
Grain-size $d^{-\frac{1}{2}}$ $mm^{-\frac{1}{2}}$	2.8		2.8
Initial dislocation density N_i, cm^{-2}	1.0×10^9		1.6×10^{10}
Initial dislocation arrangement	Random		Networks
Test Temperature	240°K	293°K	293°K
Stress-strain curve			
σ_y Kg mm^{-2}	26.8	22.2	22.6
σ_{fo} Kg mm^{-2}	19.6	14.7	19.9
K c.g.s.	8.3×10^7	8.5×10^7	3.2×10^7
n^y	0.12	0.25	0.13
Equation 3			
σ_o Kg mm^{-2}	21.6	15.0	19.0
σ_d	0.07	0.34	0.08
σ_{fo} Kg mm^{-2}	21.7	15.8	21.7
Figure 13			
σ_{fo} Kg mm^{-2}	22.5	16.4	22.4
Equation 4			
C	5.3×10^{13}	5.3×10^{11}	1.3×10^{12}
a	2.2	1.2	0.8

Table 1 (continued)

Equation 5: C'	5.3×10^{13}	5.3×10^{11}	1.9×10^{12}
a'	2.2	1.2	0.9
n/a from equation 6	0.06	0.21	0.16
n/a from Figure 13	0.07	0.17	0.15
Equation 10			
σ_o Kg mm^{-2}	7.9	7.1	7.6

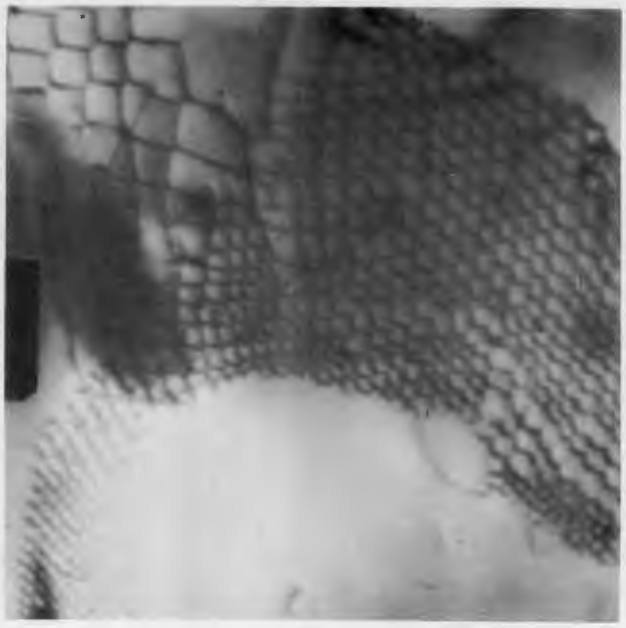

Figure 1. TaE1 Anealed 1200°C.
X50,000

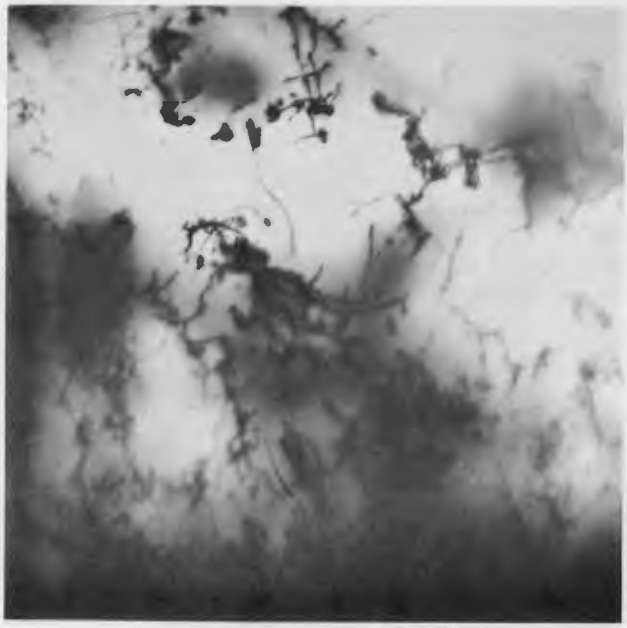

Figure 2. TaE1 Annealed 1200°C,
Deformed 7.3% in tension.
X40,000

Figure 3. TaE1 Annealed 1200°C,
Deformed 12.2% in tension.
X40,000

Figure 4. TaE4 Annealed 1750°C
Deformed 10.0% in tension
X40,000

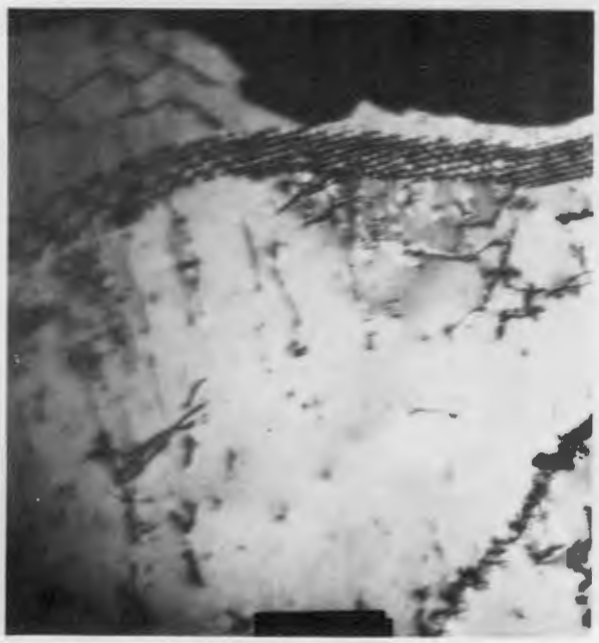

Figure 5. TaE4 Annealed 1000°C, Deformed 6.7% in Tension X40,000

Figure 6. TaE4 Annealed 1000°C, Deformed 6.7% in Tension X40,000

Figure 7. TaE1 Annealed 1200°C, Deformed 10.6% in Tension X20,000

Figure 8. TaE4 Annealed 1750°C, Deformed 4.3% in Tension X60,000

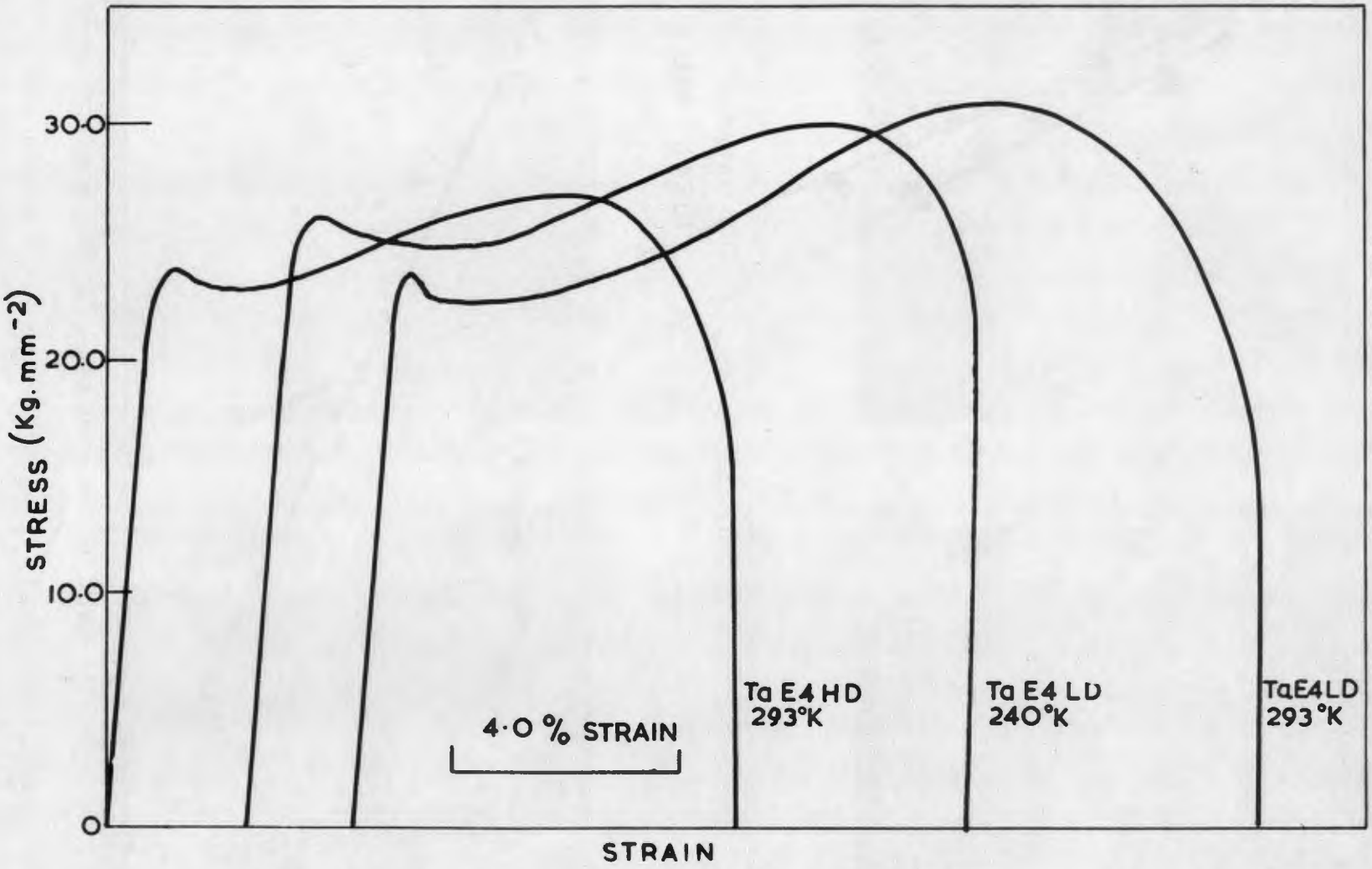

Figure 9. Experimental Stress - Strain Curves.

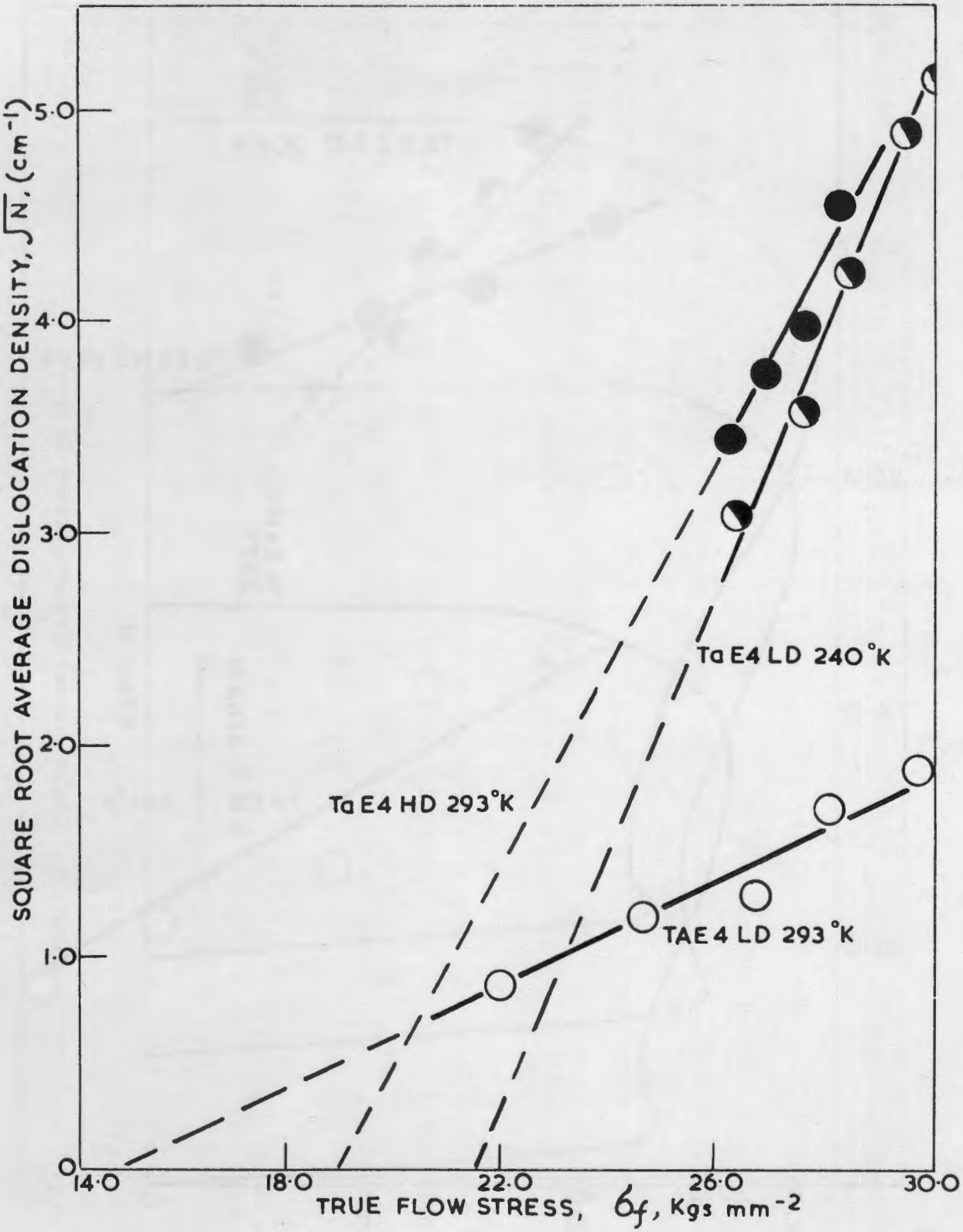

Figure 10. Dislocation Density as a Function of Flow Stress According to Equation 3.

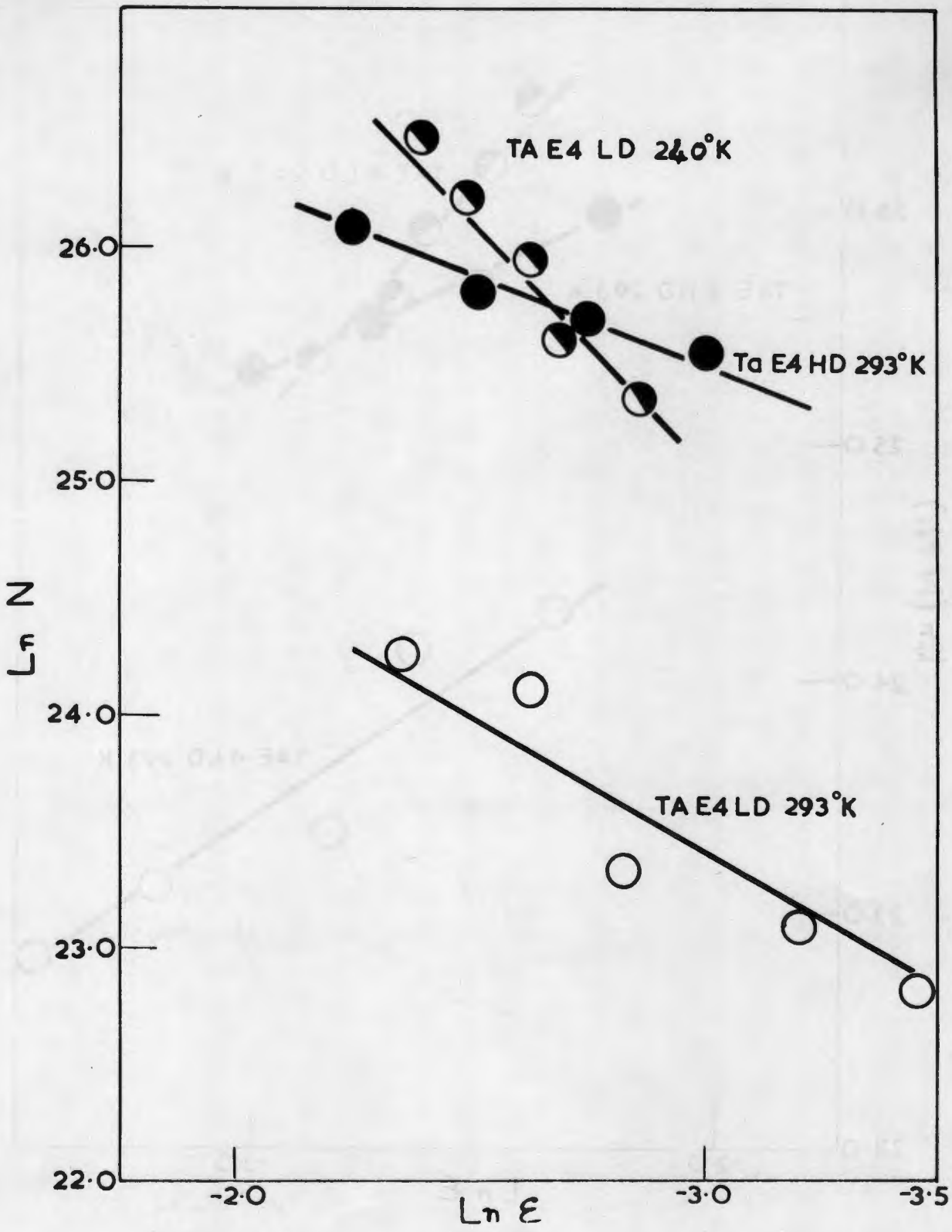

Figure 11. Dislocation Density as a Function of Strain According to Equation 4.

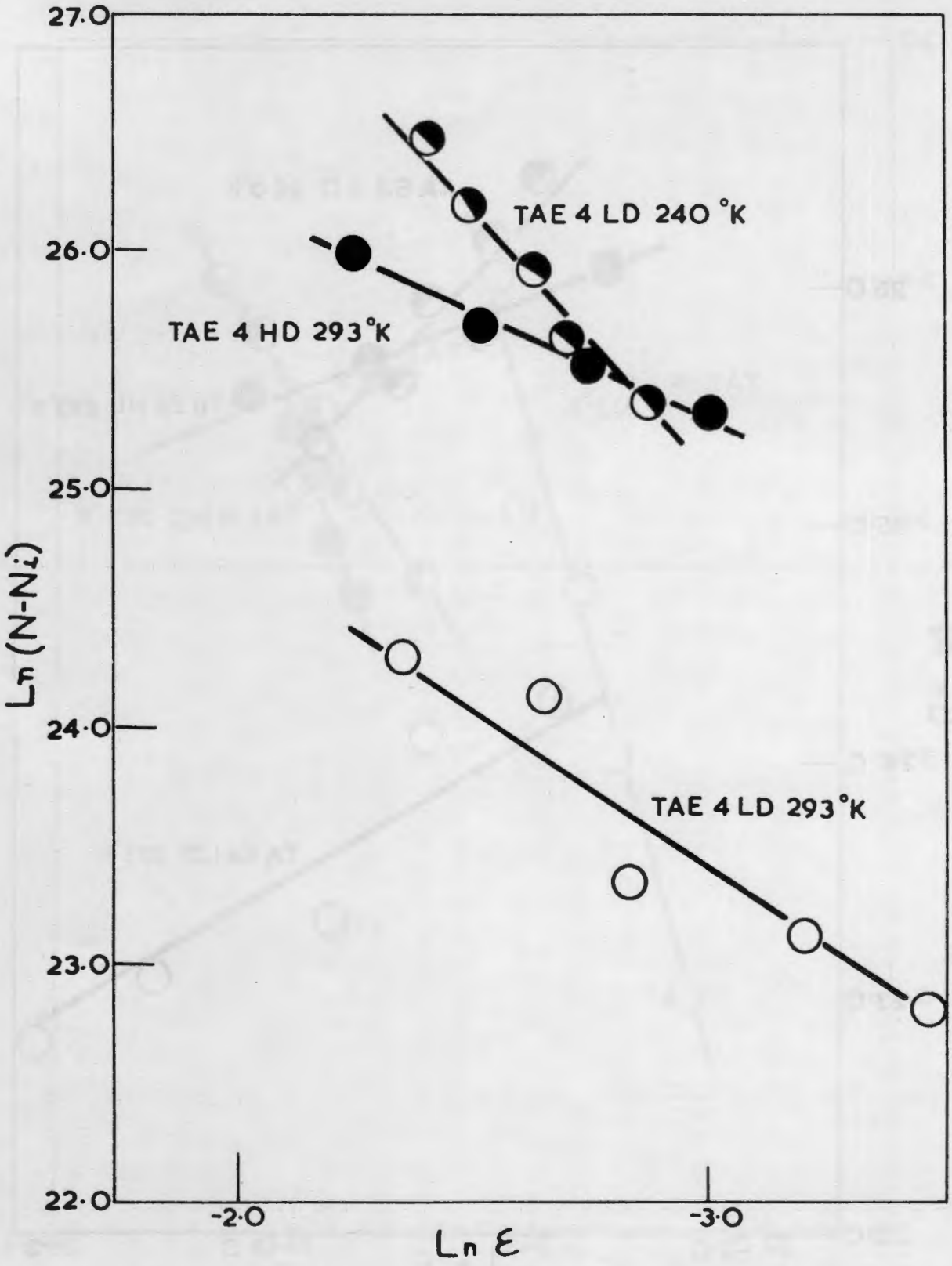

Figure 12. Dislocation Density as a Function of Strain According to Equation 5.

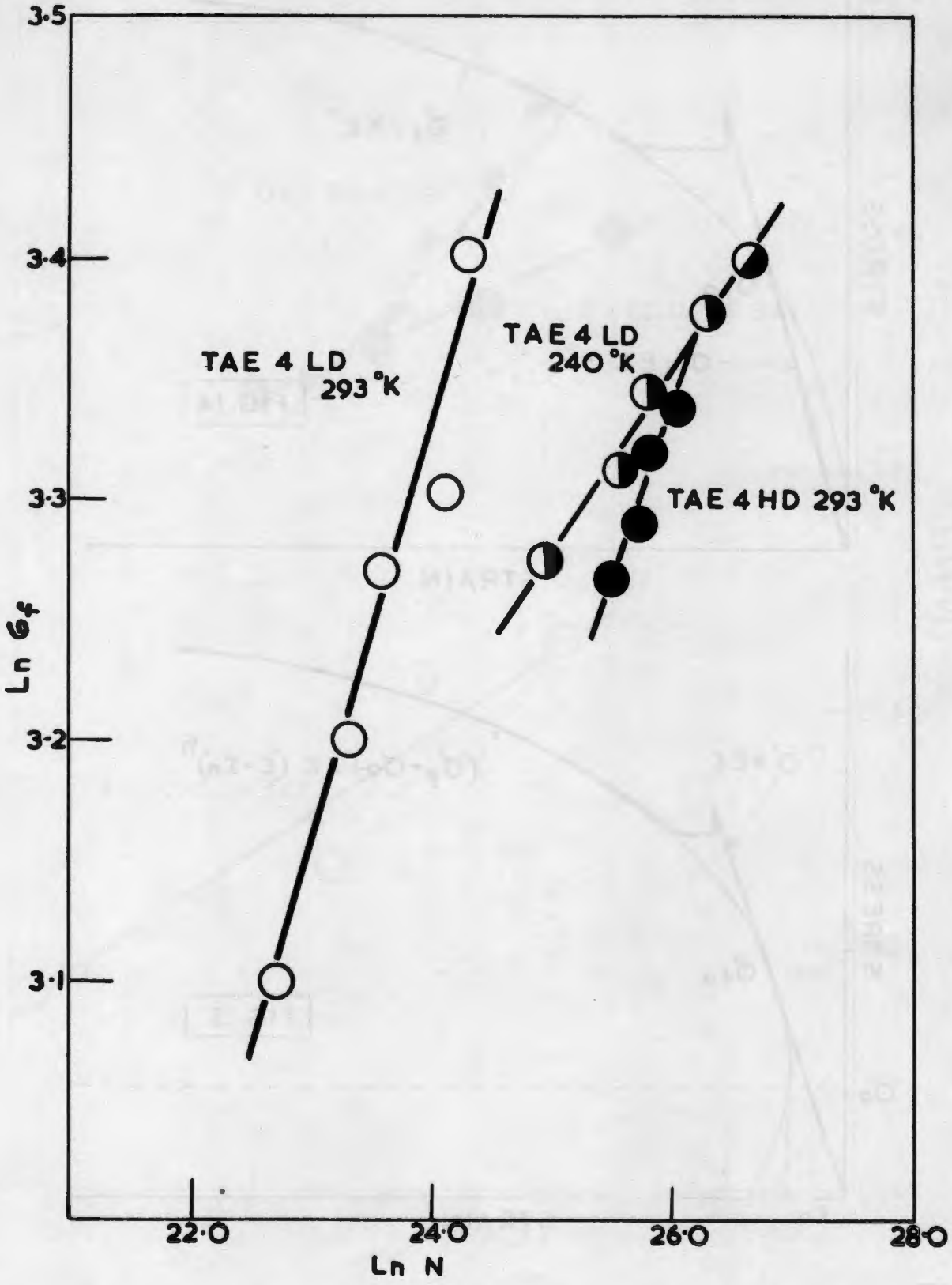

Figure 13. Flow Stress as a Function of Dislocation Density According to Equation 6.

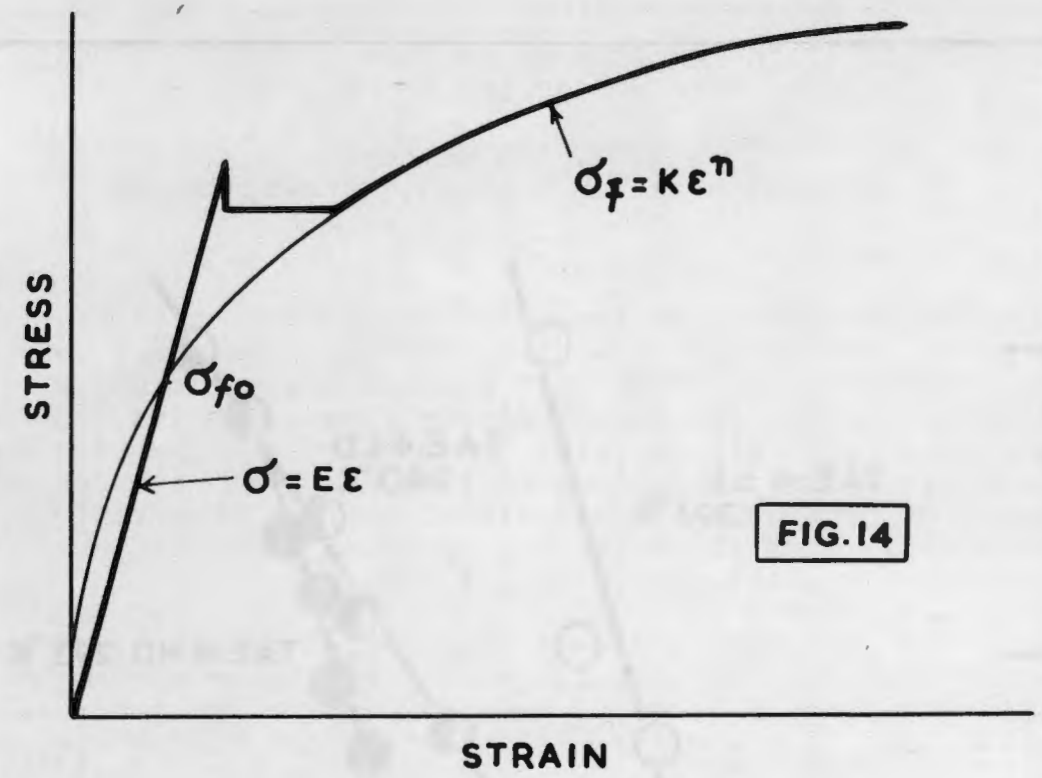

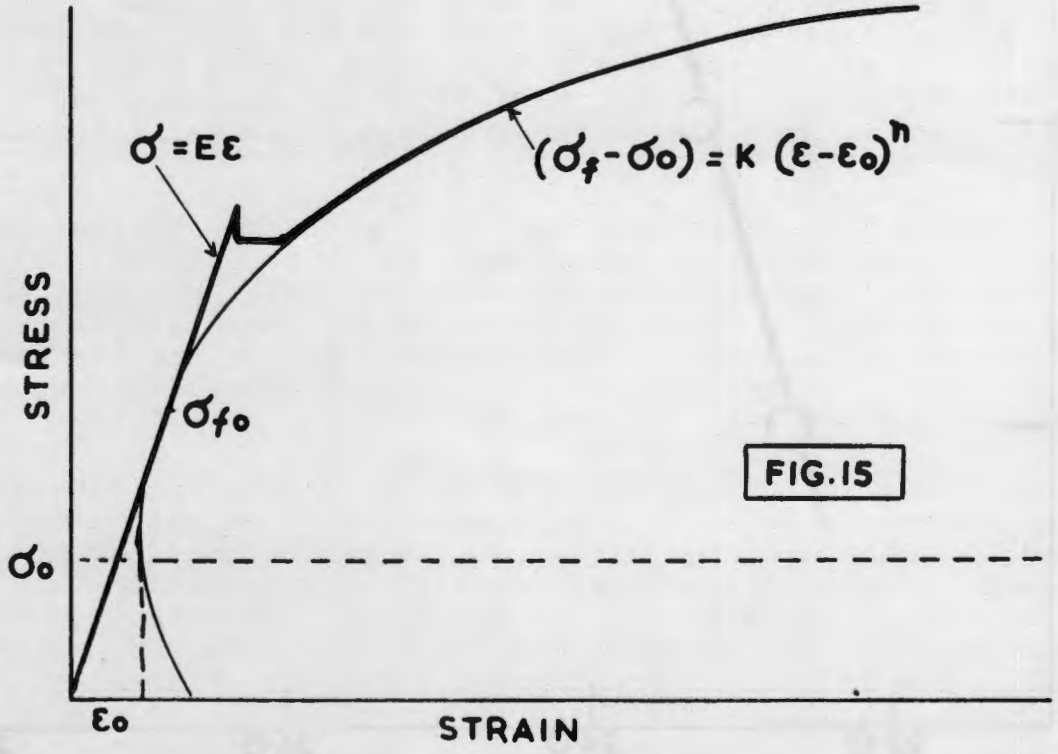

Figures 14 and 15. Schematic Stress - Strain Curve.